

## Dual Output Differential Speed and Direction Sensor IC

### FEATURES AND BENEFITS

- High-speed switching bandwidth up to 40 kHz
- Two independent output channels with options for high-resolution XOR speed, pulse, and direction protocol
- ASIL-Compliant: ASIL B SEooC developed in accordance with ISO 26262, when used as specified in the safety manual
- Immune to common external magnetic disturbance
- EEPROM enables factory traceability throughout product life cycle
- Ideally suited for asynchronous electric-motor applications
- Also available with integrated magnet (see ATS17501 datasheet)



### PACKAGE:



4-Pin SIP  
(suffix K)

Not to scale

### DESCRIPTION

The A17501 is a single IC solution designed for rotational position sensing of a ring-magnet target found in automotive and industrial electric-motor applications (often with specific application and safety requirements).

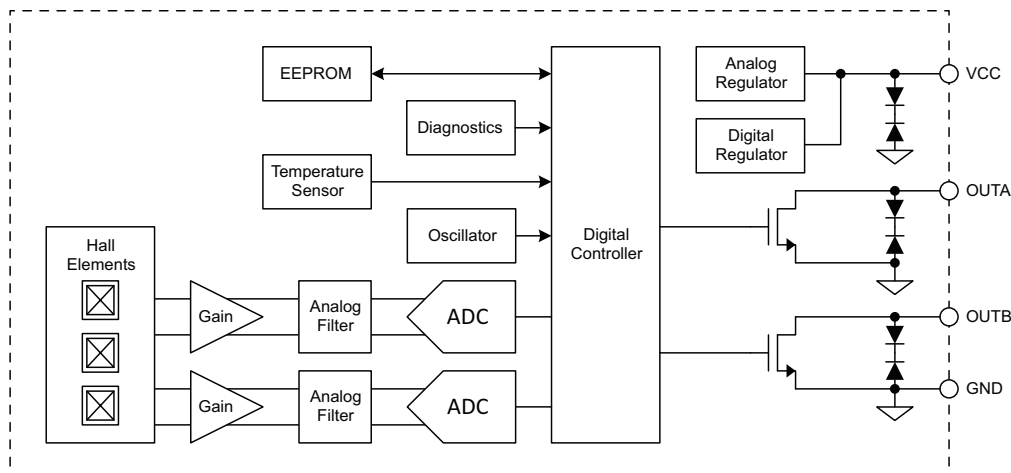
Three Hall elements are incorporated to create two independent differential channels. These inputs are processed by digital circuits and robust algorithms designed to eliminate the detrimental effects of magnetic and system offsets, and to address false output transitions caused by target vibrations in electric motors at startup and low-speed operation. The differential signals are used to produce a highly accurate speed output and, if desired, provide data about the direction of rotation.

Advanced calibration techniques are used to optimize signal offset and amplitude. This calibration, combined with digital tracking of the signal, results in accurate switch points over air gap, speed, and temperature.

The IC can be programmed for a variety of applications requiring dual-phase target speed and position signal data or simultaneous high-resolution target speed and direction data. It can be configured to enable fault-detection mode for ASILB utilization. The A17501 was developed in accordance with ISO 26262 as a hardware safety element out of context (SEooC) with ASILB capability for use in automotive safety-related systems when integrated and used in the manner prescribed in the applicable safety manual and datasheet.

The A17501 K package is a lead (Pb) free 4-pin single-inline package (SIP) with a 100% matte-tin-plated lead frame.

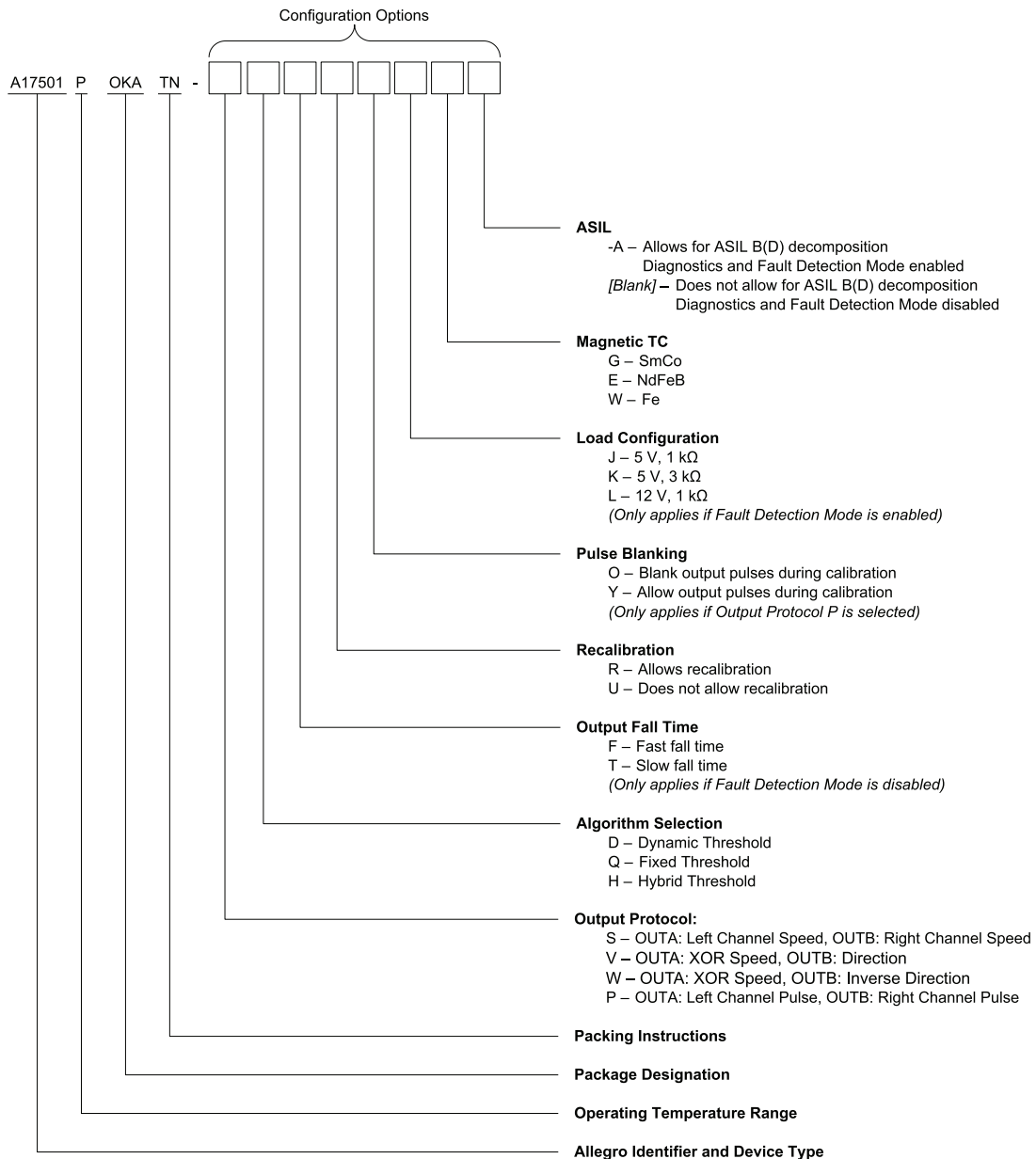
### Functional Block Diagram



## SELECTION GUIDE [1]

Part Number	Packing
A17501POKATN-SDFRYJE	4000 pieces per 13-inch reel
A17501POKATN-SDFUYJE	

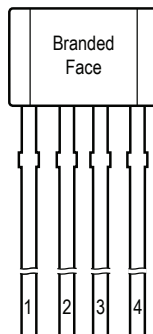
[1] Not all selectable combinations are available, contact Allegro for additional selections and packing options.



## ABSOLUTE MAXIMUM RATINGS

Characteristic	Symbol	Notes	Rating	Unit
Supply Voltage	$V_{CC}$	Refer to the Power Derating section	28	V
Reverse Supply Voltage	$V_{RCC}$		-18	V
Output Voltage	$V_{OUT}$	Each output pin	28	V
Reverse Output Voltage	$V_{ROUT}$	Each output pin; $R_{PULLUP} \geq 1\text{ k}\Omega$	-0.5	V
Output Sink Current	$I_{OUT}$	Short-term output current for OUTA and OUTB independently; not intended for continuous operation	50	mA
Operating Ambient Temperature Range	$T_A$		-40 to 160	°C
Junction Temperature	$T_J$		175	°C
Storage Temperature Range	$T_{stg}$		-65 to 170	°C

## PINOUT DIAGRAM

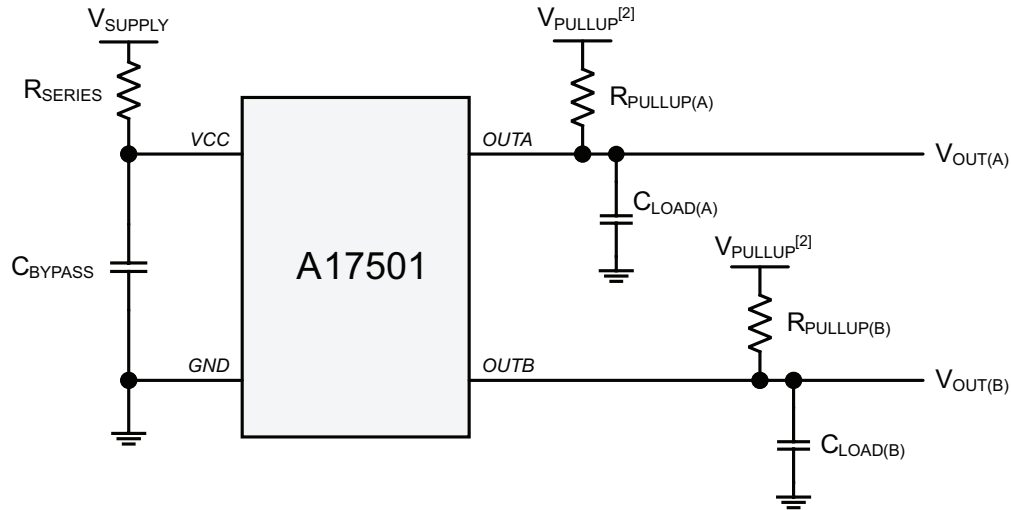


**K Package, 4-Pin SIP**

## PINOUT TABLE

Name	Pin	Function
VCC	1	Supply Voltage
OUTA	2	Configurable Output A
OUTB	3	Configurable Output B
GND	4	Ground

## TYPICAL APPLICATION CIRCUIT



## COMPONENTS [3]

Characteristic	Symbol	Notes	Value (Typ.)	Unit
Series Resistance	$R_{SERIES}$	Recommended for typical EMC requirements	100	$\Omega$
OUTA Pullup Resistance	$R_{PULLUP(A)}$	Required for functional operation; recommended value dependent on programming options	1	k $\Omega$
OUTB Pullup Resistance	$R_{PULLUP(B)}$	Required for functional operation; recommended value dependent on programming options	1	k $\Omega$
Bypass Capacitance	$C_{BYPASS}$	Recommended for typical EMC requirements	100	nF
OUTA Load Capacitance	$C_{LOAD(A)}$	Recommended for typical EMC requirements; required for certain programming options	2.2	nF
OUTB Load Capacitance	$C_{LOAD(B)}$	Recommended for typical EMC requirements; required for certain programming options	2.2	nF

<sup>[2]</sup>  $V_{PULLUP}$  may be connected to  $V_{CC}$  if  $V_{CC}$  meets  $V_{PULLUP}$  requirements. See Operating Characteristics section.

<sup>[3]</sup> Components listed are typical recommended values and are not suited for all applications and/or programmable options. See Operating Characteristics and Selection Guide for more information.

**OPERATING CHARACTERISTICS: Valid throughout operating ranges, unless otherwise specified**

Characteristic	Symbol	Test Conditions	Min.	Typ. [4]	Max.	Unit	
<b>ELECTRICAL SUPPLY CHARACTERISTICS</b>							
Supply Voltage [5]	$V_{CC}$	Voltage across VCC and GND	4	–	24	V	
Undervoltage Lockout	$V_{CC(UV)}$		–	–	3.99	V	
Supply Current	$I_{CC}$		–	10	15	mA	
Reverse Supply Current	$I_{RCC}$	$V_{CC} = -18\text{ V}$	-10	–	–	mA	
<b>ELECTRICAL PROTECTION CHARACTERISTICS</b>							
Supply Clamp Voltage	$V_{CSUPPLY}$	$T_A = 25^\circ\text{C}; I_{CC} = 18\text{ mA}$	28	–	–	V	
Reverse Supply Clamp Voltage	$V_{RCSUPPLY}$	$T_A = 25^\circ\text{C}; I_{CC} = -3\text{ mA}$	–	–	-18	V	
Output Clamp Voltage	$V_{COUT}$	$T_A = 25^\circ\text{C}; I_{OUT} = 3\text{ mA}$	28	–	–	V	
Output Current Internal Limiter	$I_{OUT(LIM)}$	Current limited by design for short-circuit event on OUTA and OUTB independently; low-impedance output state	30	55	85	mA	
<b>POWER-ON CHARACTERISTICS</b>							
Power-On State	POS	For OUTA and OUTB	$V_{OUT(HIGH)}$			V	
Power-On Time	$t_{PO}$	Time from when $V_{CC} > V_{CC(min)}$ , to when sensor IC output is valid	–	–	1	ms	
<b>CALIBRATION CHARACTERISTICS</b>							
First Output Edge	–	Amount of target rotation with constant direction following $t_{PO}$ until first electrical output transition; -xD algorithm selection; see Figure 1	–	1	2	$T_{CYCLE}$	
Initial Calibration	–	Amount of target rotation with constant direction following $t_{PO}$ until first valid speed and direction output; -xD algorithm selection; see Figure 1	–	2	4	$T_{CYCLE}$	
<b>OUTPUT CHARACTERISTICS [6]</b>							
Output Low Voltage	$V_{OUT(LOW)}$	Fault-detection mode disabled; $I_{OUT} = 10\text{ mA}$	–	0.165	0.35	V	
		Fault-detection mode enabled	5 V, 1 k $\Omega$ or 5 V, 3 k $\Omega$ option	0.5	–	1.25	V
			12 V, 1 k $\Omega$ option	1.2	–	3.6	V
Output High Voltage	$V_{OUT(HIGH)}$	Fault-detection mode disabled	–	$V_{PULLUP}$	–	V	
		Fault-detection mode enabled	5 V, 1 k $\Omega$ or 5 V, 3 k $\Omega$ option	3.75	–	4.5	V
			12 V, 1 k $\Omega$ option	8.4	–	10.8	V

Continued on next page...

[4] Typical values are for  $V_{CC} = 5\text{ V}$  and  $T_A = 25^\circ\text{C}$ , unless otherwise specified.

[5] Maximum voltage must be adjusted for power dissipation and junction temperature; see representative for Power Derating discussions.

[6] Output characteristics are valid for each output independently, unless otherwise specified.

## OPERATING CHARACTERISTICS (continued): Valid throughout operating ranges, unless otherwise specified

Characteristic	Symbol	Test Conditions	Min.	Typ. [7]	Max.	Unit	
<b>OUTPUT CHARACTERISTICS (continued) [8]</b>							
Fault Voltage [9]	$V_{\text{FAULT}}$	Fault-detection mode enabled; 5 V, 1 k $\Omega$ or 5 V, 3 k $\Omega$ option	High fault ( $V_{\text{FAULT(HIGH)}}$ )	4.5	–	–	V
			Mid fault ( $V_{\text{FAULT(MID)}}$ )	1.25	–	3.75	V
			Low fault ( $V_{\text{FAULT(LOW)}}$ )	–	–	0.5	V
		Fault-detection mode enabled; 12 V, 1 k $\Omega$ option	High fault ( $V_{\text{FAULT(HIGH)}}$ )	10.8	–	–	V
			Mid fault ( $V_{\text{FAULT(MID)}}$ )	3.6	–	8.4	V
			Low fault ( $V_{\text{FAULT(LOW)}}$ )	–	–	1.2	V
Allowable Pullup Voltage	$V_{\text{PULLUP}}$	Fault-detection mode disabled	4	–	24	V	
		Fault-detection mode enabled	5 V, 1 k $\Omega$ or 5 V, 3 k $\Omega$ option	4.75	–	5.25	V
			12 V, 1 k $\Omega$ option	11.4	–	12.6	V
Allowable Pullup Resistor [10]	$R_{\text{PULLUP}}$	Fault-detection mode disabled	–	1	–	k $\Omega$	
		Fault-detection mode enabled	5 V, 1 k $\Omega$ option	0.8	–	1.46	k $\Omega$
			5 V, 3 k $\Omega$ option	1.46	–	3.4	k $\Omega$
			12 V, 1 k $\Omega$ option	0.9	–	1.1	k $\Omega$
Allowable Load Capacitor [11]	$C_{\text{LOAD}}$	Fault-detection mode enabled	1	–	–	nF	
Output Leakage Current	$I_{\text{OUT(OFF)}}$	Fault-detection mode disabled; $V_{\text{OUT}} = V_{\text{OUT(HIGH)}}$	–	–	10	$\mu\text{A}$	
Duty Cycle	D	Sinusoidal input signal; $f_{\text{OP}} < 1$ kHz; -SD output protocol and algorithm selection	45	50	55	%	
Output Rise Time	$t_r$	10% $\rightarrow$ 90%; $V_{\text{PULLUP}} = 5$ V; $R_{\text{PULLUP}} = 1$ k $\Omega$ ; $C_{\text{LOAD}} = 2.2$ nF	–	5	–	$\mu\text{s}$	
Output Fall Time	$t_f$	90% $\rightarrow$ 10%; $V_{\text{PULLUP}} = 5$ V; $R_{\text{PULLUP}} = 1$ k $\Omega$ ; $C_{\text{LOAD}} = 2.2$ nF	Fault-detection mode disabled; fast fall-time option	–	0.5	–	$\mu\text{s}$
			Fault-detection mode disabled; slow fall-time option	–	3.5	–	$\mu\text{s}$
			Fault-detection mode enabled	–	6	–	$\mu\text{s}$
Forward Pulse Width [12]	$t_{\text{w(FWD)}}$	-P output protocol; target features pass by sensor IC branded face pin 1 to pin 4	38	45	52	$\mu\text{s}$	
Reverse Pulse Width [12]	$t_{\text{w(REV)}}$	-P output protocol; target features pass by sensor IC branded face pin 4 to pin 1	76	90	104	$\mu\text{s}$	
Propagation Delay	$t_d$	Delay from the magnetic signal crossing a switch point threshold to the start of the output transition	–	8	–	$\mu\text{s}$	
Jitter [13]	–	1 standard deviation; sinusoidal input signal; $f_{\text{OP}} = 1$ kHz	$B_{\text{DIFF(pk-pk)}} = 100$ G	–	–	0.36	% of 1 $T_{\text{CYCLE}}$
			$B_{\text{DIFF(pk-pk)}} = 150$ G	–	–	0.24	% of 1 $T_{\text{CYCLE}}$
			$B_{\text{DIFF(pk-pk)}} = 200$ G	–	–	0.18	% of 1 $T_{\text{CYCLE}}$

Continued on next page...

[7] Typical values are for  $V_{\text{CC}} = 5$  V and  $T_A = 25^\circ\text{C}$ , unless otherwise specified.

[8] Output characteristics are valid for each output independently, unless otherwise specified.

[9] Valid with fault-detection mode enabled and correct programming of the fault-detection load circuit option; see the Selection Guide.

[10] See the Typical Application Circuit section.

[11] Minimum capacitor required when fault-detection mode is enabled to ensure correct output levels over operating conditions. Increased load capacitance directly impacts the maximum operating frequency due to the increased rise and fall times; see the Typical Application Circuit section.

[12] Time from start of output transition from  $V_{\text{OUT(HIGH)}}$  to  $V_{\text{OUT(LOW)}}$  to the end of the output transition from  $V_{\text{OUT(LOW)}}$  to  $V_{\text{OUT(HIGH)}}$ . Measured pulse width varies with load circuit configurations and measurement thresholds.

[13] Guaranteed by design and characterization only. Characterization performed by measuring greater than 1,000 falling output edges at constant temperature.

**OPERATING CHARACTERISTICS (continued): Valid over operating ranges, unless otherwise specified**

Characteristic	Symbol	Test Conditions	Min.	Typ. [14]	Max.	Unit	
<b>SWITCH POINT CHARACTERISTICS</b>							
Operate Point	$B_{OP}$	% of $B_{DIFF(pk-pk)}$ ; $V_{OUT} = V_{OUT(LOW)} \rightarrow V_{OUT} = V_{OUT(HIGH)}$ ; -xD algorithm selection	–	70	–	%	
Release Point	$B_{RP}$	% of $B_{DIFF(pk-pk)}$ ; $V_{OUT} = V_{OUT(HIGH)} \rightarrow V_{OUT} = V_{OUT(LOW)}$ ; -xD algorithm selection	–	30	–	%	
Hysteresis	$B_{HYS}$	$\Delta B_{DIFF}$ after switch point to allow next output transition	% of $B_{DIFF(pk-pk)}$ ; -xD algorithm selection	–	40	–	%
			-xQ algorithm selection	–	10	–	G
<b>INPUT CHARACTERISTICS</b>							
Operating Frequency	$f_{OP}$	Fundamental frequency of the input magnetic signal	-S output protocol	0	–	40	kHz
			-V or -W output protocol	0	–	20	kHz
Forward Pulse Operating Frequency	$f_{OP(FWD)}$	-P output protocol	0	–	9	kHz	
Reverse Pulse Operating Frequency	$f_{OP(REV)}$	-P output protocol	0	–	6	kHz	
Operating Magnetic Input [15]	$B_{DIFF(pk-pk)}$	See Figure 2	-xD algorithm selection; $f_{OP} \leq 20$ kHz	30	–	–	G
			-xD algorithm selection; $f_{OP} > 20$ kHz	40	–	–	G
			-xQ algorithm selection	100	–	–	G
Operating Magnetic Input Peak [15]	$B_{DIFF}$	See Figure 2	–1150	–	1150	G	
Operating Magnetic Input Signal Variation [16]	$\Delta B_{DIFF(pk-pk)}$	Bounded amplitude ratio within $T_{WINDOW}$ ; no missed output transitions; possible incorrect direction data and/or reduction in switch-point accuracy; see Figure 3 and Figure 4	0.6	–	2	–	
Operating Magnetic Input Signal Variation Window	$T_{WINDOW}$	Rolling window in which $\Delta B_{DIFF(pk-pk)}$ cannot exceed bounded ratio; see Figure 3 and Figure 4	8	–	–	$T_{CYCLE}$	
<b>THERMAL CHARACTERISTICS</b>							
Package Thermal Resistance	$R_{\theta JA}$	Single-sided PCB, with copper limited to solder pads	–	177	–	°C/W	

[14] Typical values are for  $V_{CC} = 5$  V and  $T_A = 25^\circ\text{C}$ , unless otherwise specified.

[15] Differential magnetic field is measured for left channel (E1-E2) and right channel (E2-E3) independently; see the Package Outline Drawing section. Magnetic field is measured orthogonally to the branded package face.

[16] Operating magnetic input variation is valid for symmetrical peak variation about the signal offset.  $B_{DIFF(pk-pk)}$  must always be greater than  $B_{DIFF(pk-pk,min)}$ .

REFERENCE

Definition of Terms

$T_{CYCLE}$

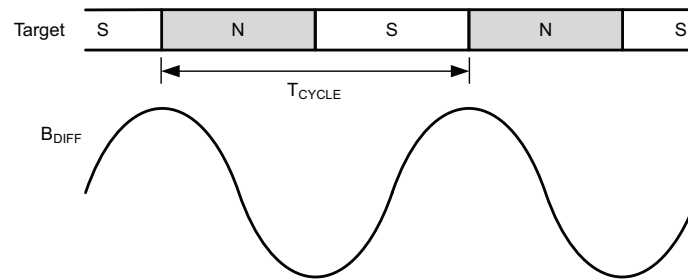


Figure 1: Definition of  $T_{CYCLE}$

$T_{CYCLE}$  = Target Cycle; the amount of rotation that moves one tooth and valley across the sensor.

$B_{DIFF}$  = The differential magnetic flux density sensed by the IC.

Differential Magnetic Input

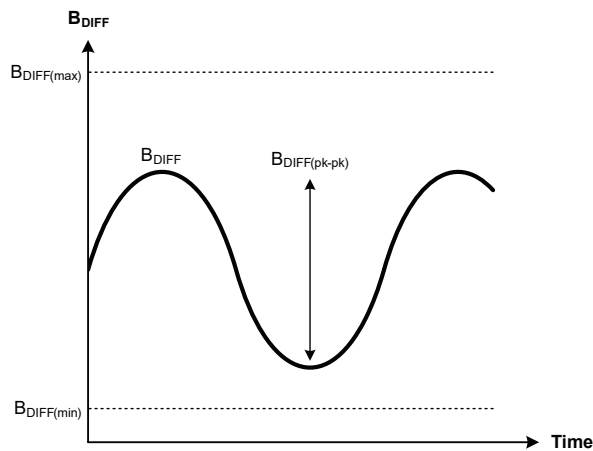


Figure 2: Differential Magnetic Input

$B_{DIFF(pk-pk)}$  = The peak-to-peak magnetic flux density sensed by the IC.

Operating Magnetic-Signal Variation and Window

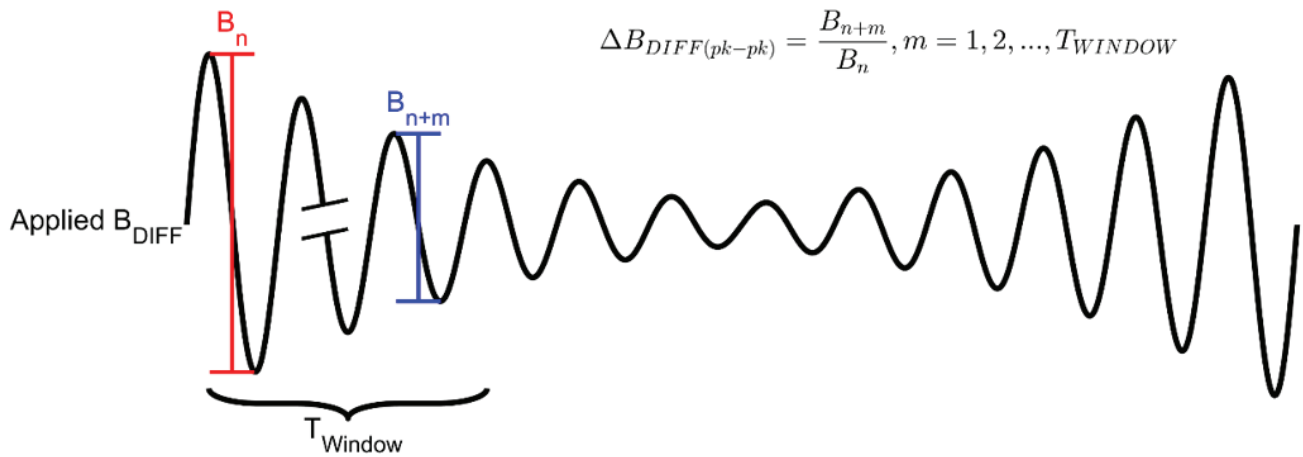


Figure 3: Repeated Period Variation

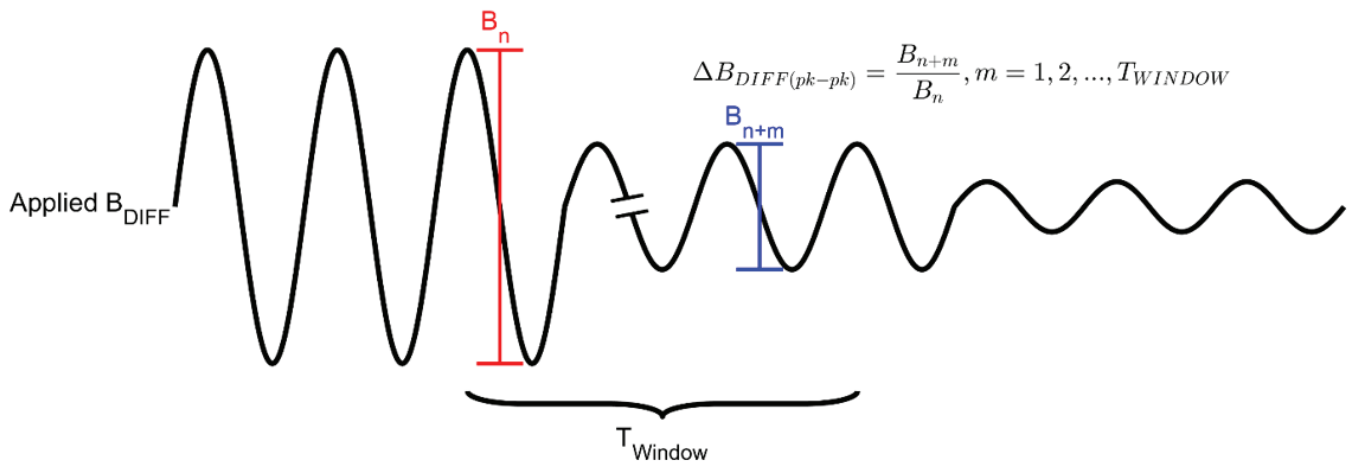
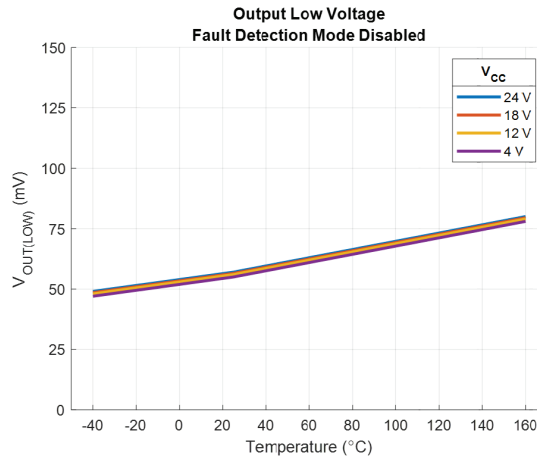
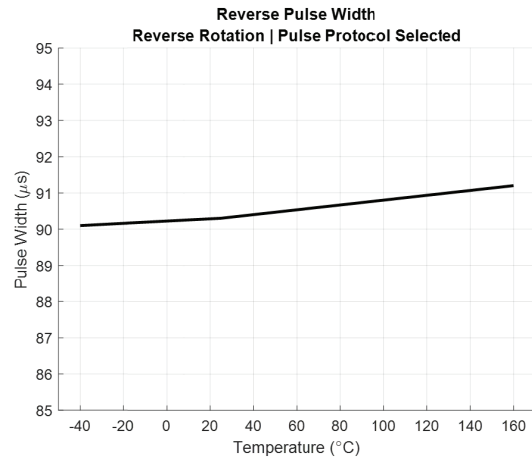
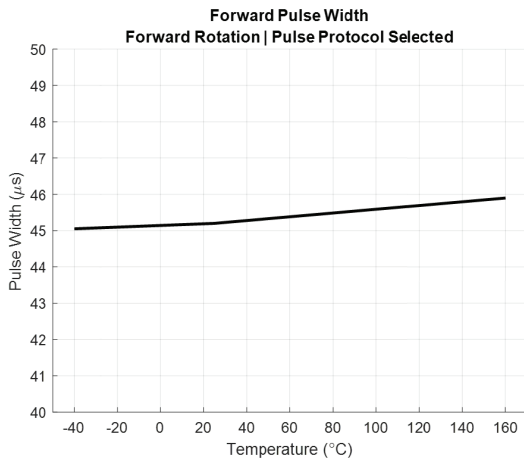
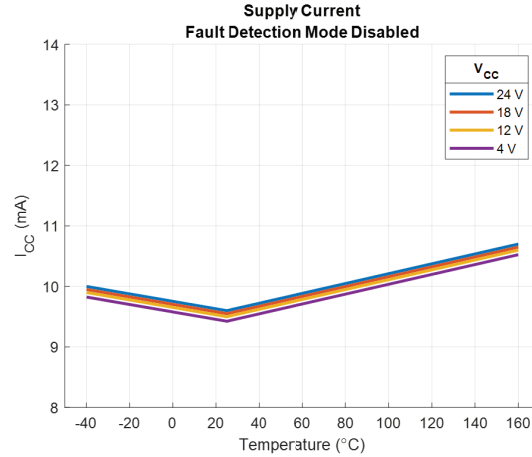
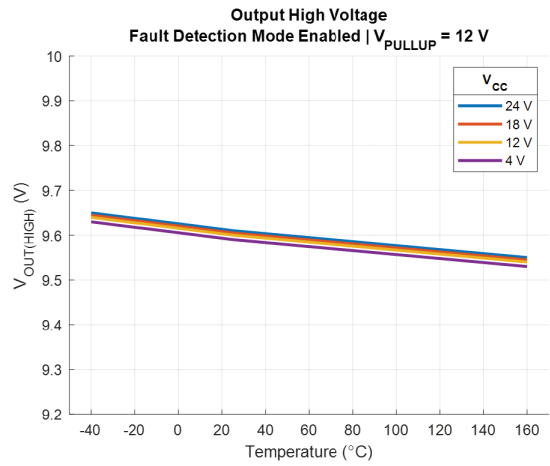
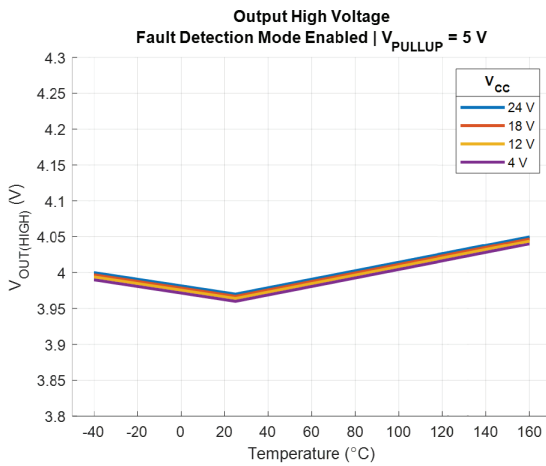
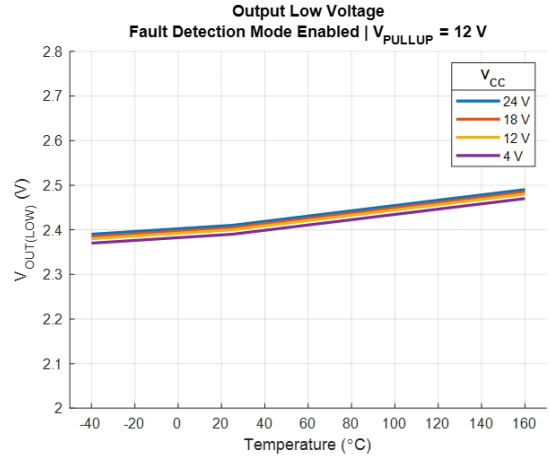
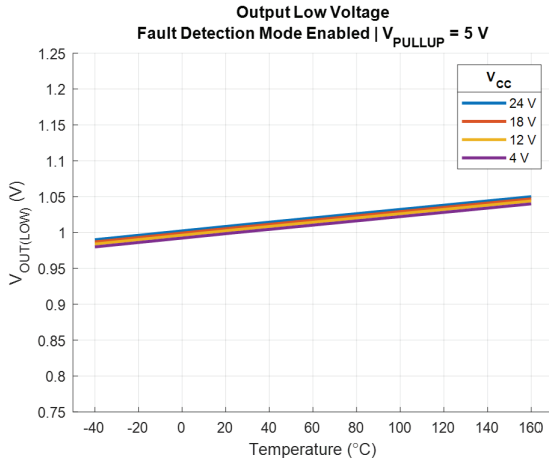


Figure 4: Single Period Variation

CHARACTERIZATION PLOTS [17]



[17] Characterization data representative of distribution averages. Characterization tested with -xD algorithm selection at  $f_{OP} = 1$  kHz,  $V_{CC} = 5$  V,  $V_{PULLUP} = 5$  V,  $R_{PUL-LUP} = 1$  k $\Omega$ , and  $C_{LOAD} = 2.2$  nF, unless otherwise specified.



## FUNCTIONAL DESCRIPTION

## General

As shown in Figure 5, the A17501 supports three Hall elements that sense the magnetic profile of the ring-magnet target simultaneously but at different points (each channel spaced at 1.75 mm pitch), generating two differential internal signals processed for precise switching of the digital output signals. The direction of rotation can be determined based on the phase relationship of the two differential internal signals. The A17501 is intended for use with ring-magnet targets, or ferromagnetic targets when properly back-biased.

The Hall-effect sensor IC is self-calibrating and possesses a temperature-compensated amplifier as well as a full-range analog-to-digital converter (ADC). This allows for accurate processing of a wide range of target magnetic-profile amplitudes and offsets. The on-chip voltage regulator provides supply-noise rejection throughout the operating voltage range. Changes in temperature do not greatly affect the A17501 due to the stable amplifier design and full-range ADC. The Hall elements and signal processing electronics are integrated on the same silicon substrate.

The A17501 is capable of providing digital data that is representative of the mechanical features of a rotating target. Automatic translation of the mechanical profile to the digital output signal is shown in Figure 5. Additional optimization is not needed, and only minimal processing circuitry is required. This ease of use reduces design time and incremental assembly costs for most applications.

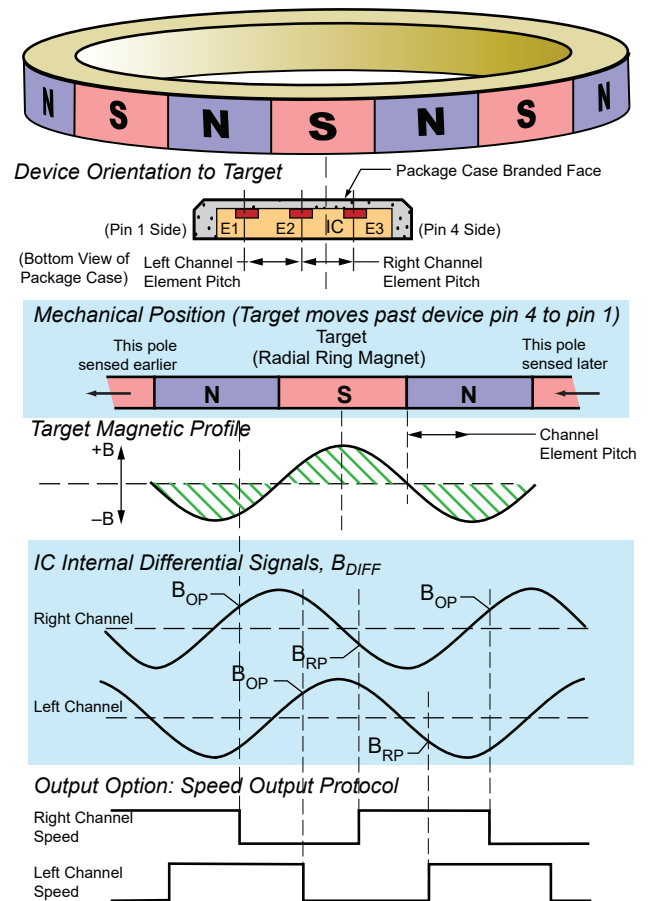


Figure 5: Magnetic Profile and Switch Points  
( $B_{OP} = 70\%$ ,  $B_{RP} = 30\%$ )

## Threshold Algorithms

The A17501 contains selectable algorithms for determining when to produce an output transition from the magnetic input signal. For all options, a threshold is set within the sensor IC that triggers the output transition when crossed by the digitized magnetic signals (switch point).

### Dynamic Threshold

With the A17501 programmed for the dynamic threshold option (-xD algorithm selection; see Figure 6), each switch point is calculated from data obtained from the previous target feature. This algorithm allows for robust tracking to produce accurate output transitions for inconsistent magnetic input signals (offset drift, amplitude changes, etc.).

After power-on, the magnetic input signal is tracked to find the peaks of the signal. After each new peak is found, the switch points are updated based on a percentage of the previous two peaks.

### Fixed Threshold

With the A17501 programmed for the fixed threshold option (-xQ algorithm selection; see Figure 7), an absolute threshold stored in memory is used to set the switch point for both the operate point and release point. This algorithm allows for accurate output transitions immediately after power-on for consistent magnetic input signals without the need to “learn” the signal. The threshold stored in memory and loaded during power-on contains threshold levels over temperature to allow for offset drift adjustment of the magnetic input signal over temperature. The A17501 sensor IC contains a temperature sensor used continuously to adjust the switch point over temperature as needed by the application.

The fixed thresholds stored in memory can be pre-programmed for unique switch points over temperature for each application. Additionally, the A17501 can find and set the threshold for each installation over temperature during end-of-line calibration.

If, during the application, the magnetic input signal offset does not match the programmed threshold stored in memory (due to inaccurate programming, mechanical shift, etc.), the A17501 identifies the threshold as out of range, calculates the threshold for the current temperature, and updates the threshold to produce correct output transitions. After the update, algorithms use the current temperature to recharacterize the threshold over the operational temperature range. This prevents the update from overcompensating the threshold at a distant temperature relative to the update temperature. After the updated threshold is confirmed to be within the magnetic input signal’s switch point range over several target features, the updated threshold is stored into memory such that it can be used for subsequent power-on cycles.

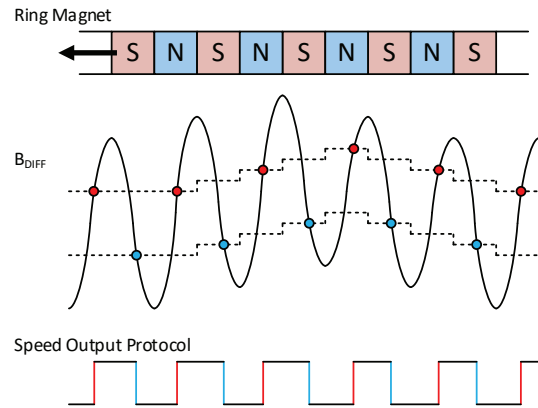


**Figure 6: Dynamic Threshold Option Switch Point Algorithm ( $B_{OP} = 70\%$ ,  $B_{RP} = 30\%$ )**

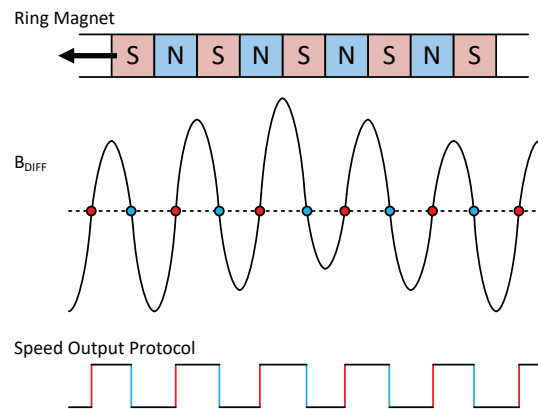


**Figure 7: Fixed Threshold Option Switch Point Algorithm**

### *Hybrid Threshold*

With the A17501 programmed for the hybrid-threshold option (-xH algorithm selection), the threshold is determined from the fixed-threshold option at startup, then transitions to the dynamic-threshold option after tracking signals have correctly acquired the magnetic input signals. This algorithm allows for both accurate output transitions immediately following power-on for consistent magnetic input signals as well as robust tracking to produce accurate output transitions of inconsistent magnetic input signals (offset drift, amplitude changes, etc.).

Once the tracking signals have identified consistent peak values from the magnetic input signal, the algorithm transitions from using the fixed-threshold switch point to using the dynamic-threshold switch points. This transition occurs only when the magnetic input signal is near a maximum or minimum value, such that double-switching can be avoided during the transition.

While the majority of the power-on uses the dynamic-threshold option for robust signal tracking, the A17501 continues to monitor the fixed threshold for comparison to the fixed threshold stored in memory. Should the fixed threshold require an update, the A17501 updates and writes the new threshold to memory, for use in subsequent power-on cycles.

Output

Output Protocol

The A17501 contains several selectable options to change the output protocol or adjust the output behavior. These options allow for the A17501 to be programmed to application-level needs; see Figure 8. If the datasheet output protocol options are not quite fit for the application, consult Allegro MicroSystems about custom sensor programmability.

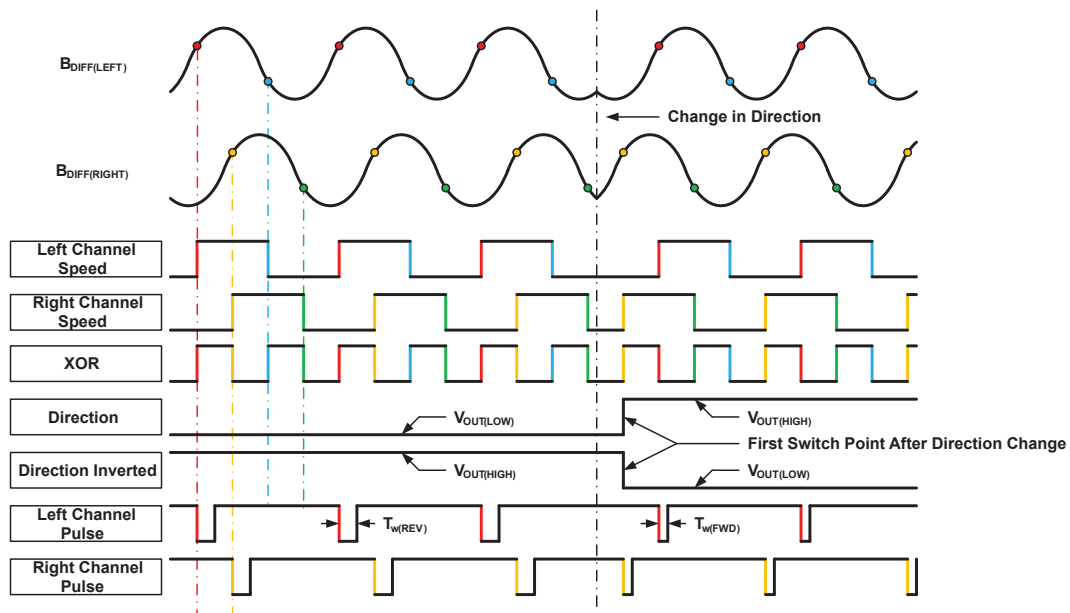


Figure 8: Output Protocol Options

**Fault-Detection Mode**

The A17501 allows for the output to transition between one of two sets of values. With fault-detection mode disabled, the output transitions between approximately 0% and 100% of  $V_{PULLUP}$  (see Figure 9). With fault-detection mode disabled, the output transitions between approximately 20% and 80% of  $V_{PULLUP}$ .

At the beginning of power-on, the A17501 outputs initialize to the  $V_{PULLUP}$  level. With fault-detection mode enabled, the output levels transition from  $V_{PULLUP}$  to  $V_{HIGH}$  before the end of power-on (see Figure 10). After power-on, the output transitions as determined by the programmed algorithm and output protocol between  $V_{OUT(HIGH)}$  and  $V_{OUT(LOW)}$ .

Enabling fault-detection mode allows for additional communication for cases of open wire or short circuit, as well as allowing for the A17501 to communicate a fault detected from the internal diagnostics. For a typical application load circuit, these cases can be detected by observing either OUTA or OUTB transition to approximately 0 V or  $V_{PULLUP}$  after  $t_{PO}$ .

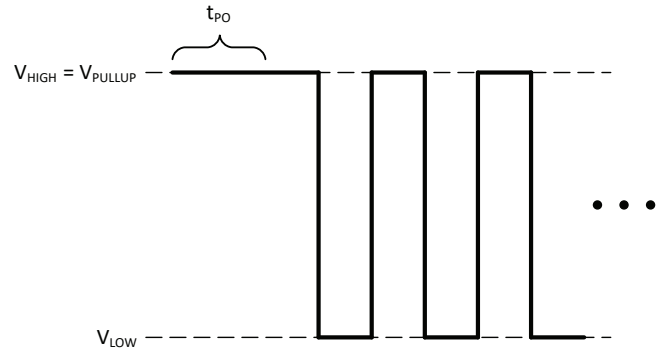


**Figure 9: Fault-Detection Mode Disabled Output**

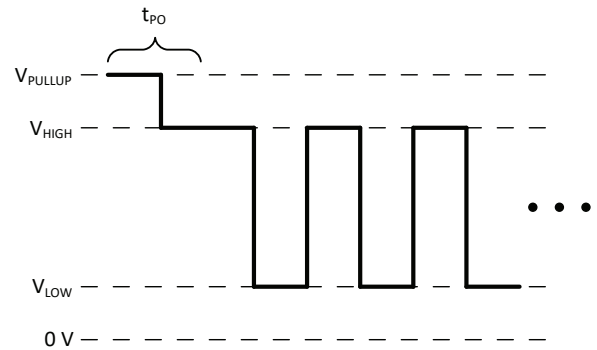


**Figure 10: Fault-Detection Mode Enabled Output**

**Fault Voltage**

The A17501 communicates a fault condition by configuring either output to hold within one of three  $V_{FAULT}$  ranges (high, mid, and low) for greater than 1 millisecond. Typical operation allows for output transitions to occur over the  $V_{FAULT(MID)}$  range; as such, it is necessary to ignore fast transients for less than 1 millisecond through this range.

For internal diagnostics that trigger fault conditions (force the output to go to  $V_{FAULT}$ ), both outputs transition to the  $V_{FAULT(HIGH)}$  range. Because there may exist internal or external faults that cause either or both output pins to hold a  $V_{FAULT(MID)}$  or  $V_{FAULT(LOW)}$  level, these fault ranges should also be monitored. Examples of these fault conditions could be a short circuit of the output to ground, forcing the output to  $V_{FAULT(LOW)}$ , or a fault in the IC output controller that forces the output to  $V_{FAULT(MID)}$ .

For examples of the output communicating a fault condition, see Figure 11, Figure 12, and Figure 13.

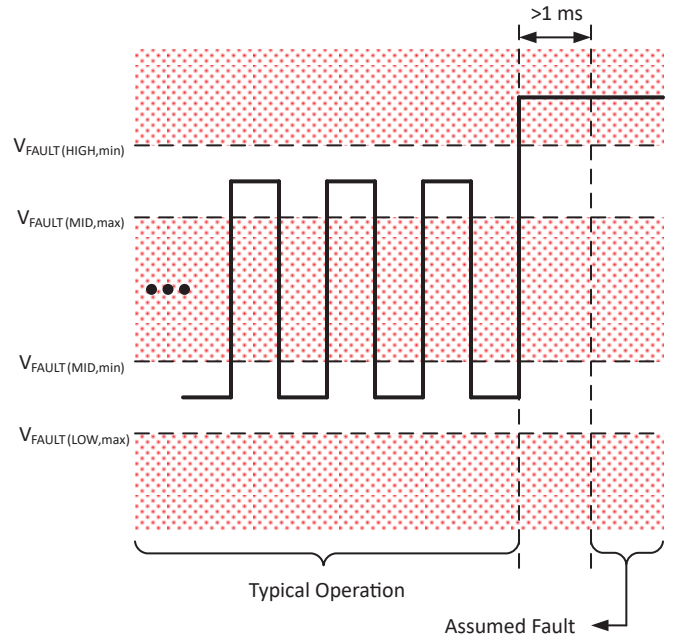


**Figure 11: Assumed Fault Example: High Fault**

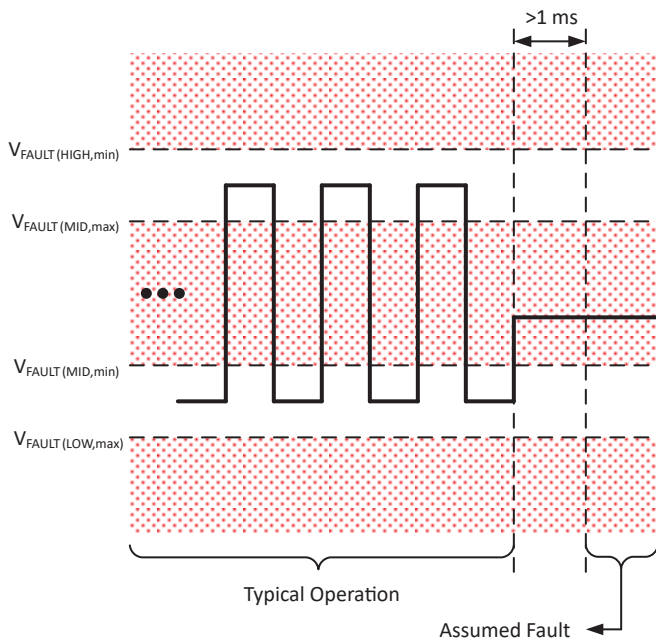


**Figure 12: Assumed Fault Example: Mid Fault**

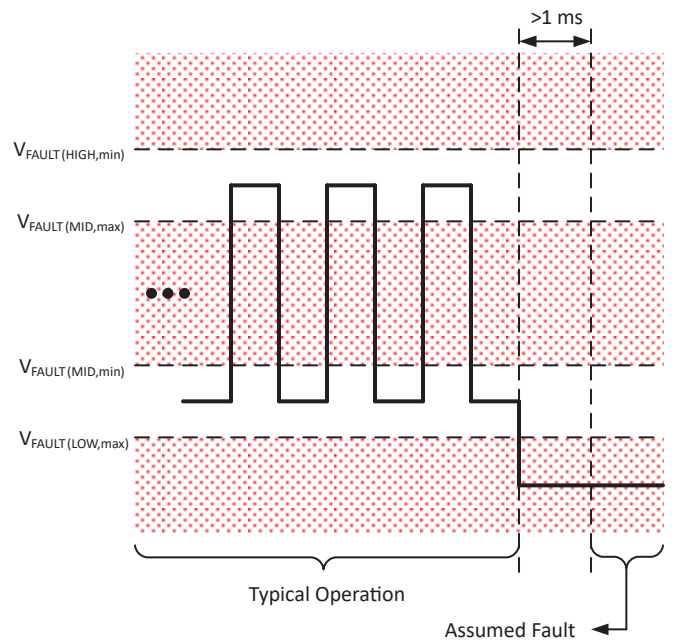


**Figure 13: Assumed Fault Example: Low Fault**

## DEVICE FEATURES

### *Undervoltage Lockout*

When supply voltage reduces to less than the undervoltage lockout voltage ( $V_{CC(UV)}$ ), the A17501 enters reset, where the output state returns to the power-on state (POS) until sufficient  $V_{CC}$  is supplied. This feature prevents false signals, caused by undervoltage conditions, from propagating to the output of the sensor IC.

### *Power-Supply Protection*

The A17501 contains an on-chip regulator and can operate over a wide  $V_{CC}$  range. For applications that need to operate from an unregulated power supply, transient protection must be added externally. For applications using a regulated line, electromagnetic interference (EMI)/radio-frequency interference (RFI) protection is recommended. For more information about circuitry to address electromagnetic-compatibility (EMC) requirement compliance, contact Allegro. Refer to the Typical Application Circuit section.

### *Startup Hysteresis*

With a power-on and a target held at zero-speed ( $f_{OP} \approx 0$  Hz), noise and/or vibration can produce magnetic input signals. Startup hysteresis prevents peak-tracking and switch-point setting at startup immediately following power-on. This occurs until the sensed differential magnetic signal has moved sufficiently to satisfy the hysteresis band for signal tracking. This feature helps to ensure optimal self-calibration of the magnetic signals by rejecting electrical noise and low-amplitude target vibrations during startup and ensures that calibration occurs on actual target features.

### *Small-Signal Lockout*

When  $B_{DIFF(pk-pk)}$  reduces to less than the specification, the internal logic of the sensor IC indicates a reduced signal, as measured in an excessive air gap or a vibration condition. Small-signal lockout holds the output state at the level when  $B_{DIFF(pk-pk)}$  was last in-specification. Once  $B_{DIFF(pk-pk)}$  returns to an in-specification value, the output state is released to transition as expected during typical operation. When direction data is not explicitly defined by the selected output protocol, the small-signal lockout is controlled independently for each channel. For example, left-channel speed + right-channel speed output protocol allows for one channel to continue switching while the other is in lockout. When direction data is explicitly communicated, for example XOR + direction output protocol, the small-signal lockout occurs when the  $B_{DIFF(pk-pk)}$  of either channel reduces to less than specification.

### *Vibration-Robust Signal Tracking*

During vibration events, the magnetic input signals can produce oscillations with a sufficient amplitude for the peak-tracking algorithms to bound in and produce a nonideal peak-to-peak. When the A17501 detects a direction change, inward bounding of the peak-tracking signals is prevented. This prevents cases of erroneous output transitions from switch points being incorrectly set from vibration signals. Additionally, this allows for immediate acquisition of the magnetic input signals once real target rotation resumes following a vibration event.

### *Signature-Region-Robust Signal Tracking*

Signature teeth (characterized by an extra target tooth and/or valley) can produce significant variations of the magnetic input signals. The bounded updating of the tracking signals prevents overcompensation for these signature variations to provide robust and accurate switch points for the signature region, as well as the features about the signature region.

### *Temperature-Drift-Robust Signal Tracking*

Because temperature changes can impact both the amplitude and offset of the magnetic signal, a full-range ADC, advanced algorithms, temperature compensation, watchdog timers, and internal temperature sensor ensure robust signal tracking over temperature.

To compensate for amplitude changes over temperature, temperature-compensated gain is first applied to normalize the amplitude over temperature. The full-range ADC and peak-tracking algorithms track and acquire the signal to accurately set the switch points.

To compensate for the offset changes over temperature, two algorithms are implemented to ensure the signal tracking accurately follows and updates the switch points to follow the offset. With typical target rotation, peak-tracking algorithms automatically follow and update the switch points over offset drift. With no target rotation (stopped condition), a watchdog timer is implemented, which adjusts the algorithms to track together, allowing for preservation of the correct signal peak-to-peak and switch points once rotation resumes.

With the fixed-threshold algorithm option selected, algorithms are implemented for continuous monitoring and updating of the fixed threshold over temperature to follow the offset drift of the system. This compensation is implemented for each channel independently to provide robust tracking of both signal channels over temperature.

### *Diagnostics and Fault Reporting*

The A17501 contains diagnostics monitors of analog and digital circuits of the IC. These continuously monitor and report if any defect, calculation error, or invalid input stimulus is found. If a diagnostic monitor activates, the outputs of the A17501 transition to a  $V_{\text{FAULT}}$  level. For all faults, the outputs remain at the  $V_{\text{FAULT}}$  level for enough time to allow the system controller to monitor that a fault has occurred. For some diagnostics, it is possible to clear the fault with a reset of the internal controller of the sensor IC. If any of those diagnostic monitors triggers the fault event, the A17501 automatically performs a reset of the internal controller after the output is held at  $V_{\text{FAULT}}$  for enough time to allow the system controller to monitor the fault event.

Proper performance of diagnostics and fault reporting requires proper programming and adherence to the specifications and assumptions stated in this datasheet, the A17501 Safety Manual, and any other addendum, corrigendum, and application note that applies to the A17501. For more information about diagnostics and fault reporting, see the A17501 Safety Manual.

### *Recalibration*

Under large amplitude vibration conditions at startup, the peak-to-peak and phase relationship of the magnetic input signals can meet the conditions to calibrate. Once typical rotation resumes, the actual signal amplitudes can be much larger than the peak signals acquired during calibration. Rather than wait several  $T_{\text{CYCLE}}$  events for the peak signal to be tracked to actual levels, the A17501 detects the difference and recalibrates on the new signal. Recalibration allows for fast and robust correction from cases of calibration on vibration events.

### *Pulse-Collision Prevention*

In cases of “high-speed” vibration, output transitions can occur at very high frequencies, to prevent pulse collision (truncation of the pulse width), the A17501 prevents output transitions until the current output-pulse transition is complete to ensure the system controller can accurately interpret the output signal. This feature is only implemented when a pulse protocol option is selected.

### *High Configurability*

The A17501 contains programmable parameters, as shown in the Selection Guide, that can be configured to provide application-level optimization.

**POWER DERATING**

The device must be operated at less than the maximum junction temperature of the device ( $T_{J(max)}$ ). Under certain combinations of peak conditions, reliable operation may require derating supplied power or improving the heat dissipation properties of the application. This section presents a procedure for correlating factors affecting operating  $T_J$ . (Thermal data is also available on the Allegro MicroSystems website.)

The package thermal resistance ( $R_{\theta JA}$ ) is a figure of merit summarizing the ability of the application and the device to dissipate heat from the junction (die), through all paths to the ambient air. Its primary component is the effective thermal conductivity (K) of the printed circuit board, including adjacent devices and traces. Radiation from the die through the device case ( $R_{\theta JC}$ ) is a relatively small component of  $R_{\theta JA}$ . Ambient air temperature ( $T_A$ ) and air motion are significant external factors, damped by overmolding.

The effect of varying power levels (power dissipation or  $P_D$ ), can be estimated. The following formulas represent the fundamental relationships used to estimate  $T_J$ , at  $P_D$ .

Equation 1:  $P_D = V_{IN} \times I_{IN}$

Equation 2:  $\Delta T = P_D \times R_{\theta JA}$

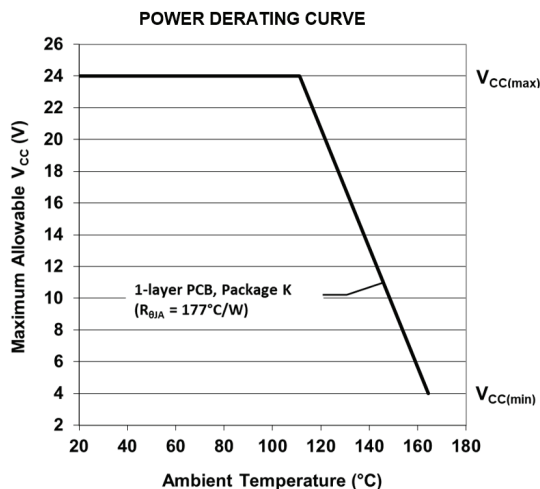
Equation 3:  $T_J = T_A + \Delta T$

For example, given common conditions, such as:  $T_A = 25^\circ C$ ,  $V_{CC} = 12 V$ ,  $I_{CC(avg)} = 8.5 mA$ , and  $R_{\theta JA} = 177^\circ C/W$ , then:

$$P_D = V_{CC} \times I_{CC(avg)} = 12 V \times 8.5 mA = 102 mW$$

$$\Delta T = P_D \times R_{\theta JA} = 102 mW \times 177^\circ C/W = 18.1^\circ C$$

$$T_J = T_A + \Delta T = 25^\circ C + 18.1^\circ C = 43.1^\circ C$$



A worst-case estimate,  $P_{D(max)}$ , represents the maximum allowable power level ( $V_{CC(max)}$ ,  $I_{CC(max)}$ ), without exceeding  $T_{J(max)}$ , at a selected  $R_{\theta JA}$  and  $T_A$ .

For example, calculating reliability of  $V_{CC}$  given observed worst-case ratings, specifically:

$$T_A = 160^\circ C, R_{\theta JA} = 177^\circ C/W, T_{J(max)} = 175^\circ C, V_{CC(max)} = 24 V, \text{ and } I_{CC(max)} = 15 mA.$$

The maximum allowable power,  $P_{D(max)}$ , can be calculated by first inverting Equation 3 and calculating the maximum allowable increase to  $T_J$ :

$$\Delta T_{max} = T_{J(max)} - T_A = 175^\circ C - 160^\circ C = 15^\circ C$$

Then, maximum allowable power can be calculated by:

$$P_{D(max)} = \Delta T_{max} \div R_{\theta JA} = 15^\circ C \div 177^\circ C/W = 84.7 mW$$

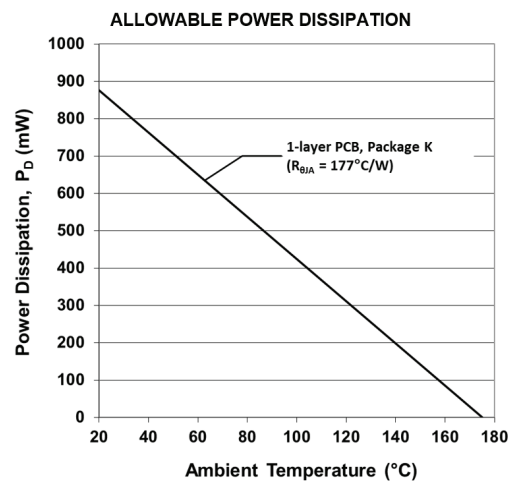
Finally, invert Equation 1 with respect to voltage:

$$V_{CC(est)} = P_{D(max)} \div I_{CC(max)} = 84.7 mW \div 15 mA = 5.65 V$$

The results indicate that, at  $T_A$ , the application and A17501 can dissipate adequate amounts of heat at voltages less than or equal to  $V_{CC(est)}$ .

Compare  $V_{CC(est)}$  to  $V_{CC(max)}$ :

- If  $V_{CC(est)} \leq V_{CC(max)}$ , reliable operation between  $V_{CC(est)}$  and  $V_{CC(max)}$  requires enhanced  $R_{\theta JA}$ .
- If  $V_{CC(est)} \geq V_{CC(max)}$ , operation between  $V_{CC(est)}$  and  $V_{CC(max)}$  is reliable under these conditions.



PACKAGE OUTLINE DRAWING

For Reference Only – Not for Tooling Use

(Reference DWG-0000395)

Dimensions in millimeters – NOT TO SCALE

Dimensions exclusive of mold flash, gate burrs, and dambar protrusions  
Exact case and lead configuration at supplier discretion within limits shown

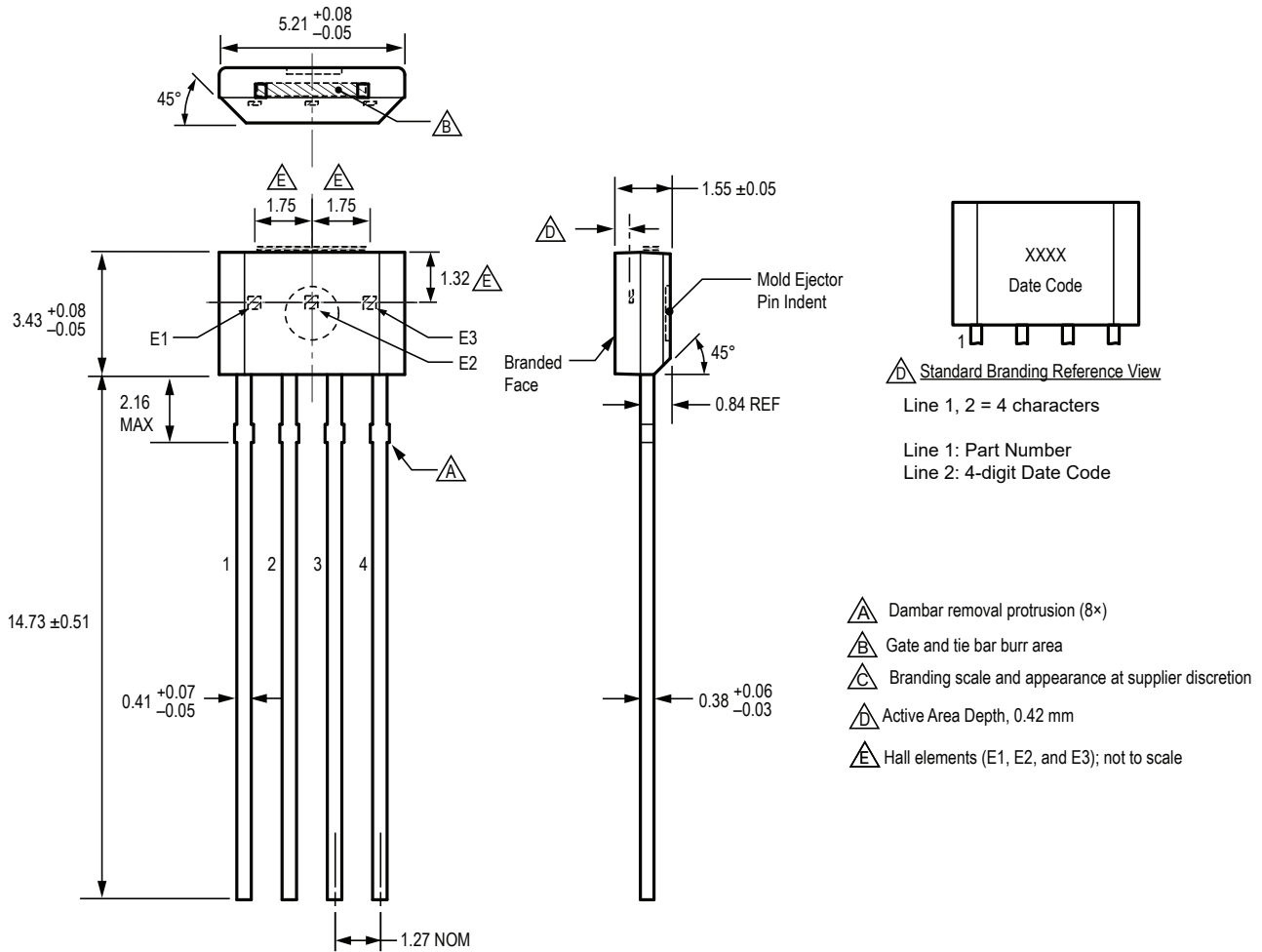


Figure 14: Package K, 4-Pin SIP

## Revision History

Number	Date	Description
–	March 19, 2020	Initial release
1	February 22, 2021	Removed Advance Information status; updated Selection Guide; minor editorial updates
2	February 22, 2024	Removed “assessment pending” (page 1); updated First Output Edge and Initial Calibration test conditions, maximum values, and footnote 4 (page 5); updated Duty Cycle, Forward Pulse Width, and Jitter test conditions, Jitter units and maximum values, and footnotes 12-13 (page 6); updated Operate Point, Release Point, Hysteresis, Operating Frequency, Forward Pulse Operating Frequency, Reverse Pulse Operating Frequency, Operating Magnetic Input test conditions and Operating Frequency values (page 7); updated Jitter plot and footnote 17 (page 10); updated Output section (page 15); updated Figure 11 (page 17); other minor editorial updates.
3	May 8, 2025	Changed ASIL logos and ASIL descriptions for clarity (page 1), modified characterization plots (page 10), and made minor editorial changes throughout (all pages).

Copyright 2025, Allegro MicroSystems.

Allegro MicroSystems reserves the right to make, from time to time, such departures from the detail specifications as may be required to permit improvements in the performance, reliability, or manufacturability of its products. Before placing an order, the user is cautioned to verify that the information being relied upon is current.

Allegro’s products are not to be used in any devices or systems, including but not limited to life support devices or systems, in which a failure of Allegro’s product can reasonably be expected to cause bodily harm.

The information included herein is believed to be accurate and reliable. However, Allegro MicroSystems assumes no responsibility for its use; nor for any infringement of patents or other rights of third parties which may result from its use.

Copies of this document are considered uncontrolled documents.

For the latest version of this document, visit our website:

[www.allegromicro.com](http://www.allegromicro.com)